BIOCHEMISTRY

 Volume 44, Number 28 July 19, 2005

Articles

Characterization of Protein Kinase C θ Activation Loop Autophosphorylation and the Kinase Domain Catalytic Mechanism

Robert Czerwinski,[‡] Ann Aulabaugh,[‡] Rita M. Greco,[§] Stephane Olland,[||] Karl Malakian,[‡] Scott Wolfrom,[‡] Laura Lin,[‡] Ron Kriz,[‡] Mark Stahl,[‡] Ying Huang,[||] Lin Liu,[||] and Divya Chaudhary*[,§]

Departments of Chemical and Screening Sciences, Inflammation, and Protein Technologies, Wyeth Research, 87 Cambridge Park Drive, Cambridge, Massachusetts 02140

Received April 1, 2005; Revised Manuscript Received May 20, 2005

ABSTRACT: Protein kinase C θ (PKCθ), a member of the Ca^{2+}-independent novel subfamily of PKCs, is required for T-cell receptor (TCR) signaling and IL2 production. PKCθ-deficient mice have impaired Th2 responses in a murine ova-induced asthma model, while Th1 responses are normal. As an essential component of the TCR signaling complex, PKCθ is a unique T-cell therapeutic target in the specific treatment of T-cell-mediated diseases. We report here the PKCθ autophosphorylation characteristics and elucidation of the catalytic mechanism of the PKCθ kinase domain using steady-state kinetics. Key phosphorylated residues of the active PKCθ kinase domain expressed in *Escherichia coli* were characterized, and mutational analysis of the kinase domain was performed to establish the autophosphorylation and kinase activity relationships. Initial velocity, product inhibition, and dead-end inhibition studies provided assignments of the kinetic mechanism of $PCK\theta_{362-706}$ as ordered, wherein ATP binds kinase first and ADP is released last. Effects of solvent viscosity and ATPγS on PKCθ catalysis demonstrated product release is partially rate limiting. Our studies provide important mechanistic insights into kinase activity and phosphorylation-mediated regulation of the novel PKC isoform, PKCθ. These results should aid the design and discovery of PKCθ antagonists as therapeutics for modulating T-cell-mediated immune and respiratory diseases.

PKCθ[1] belongs to the Ca^{2+}-independent novel subfamily of PKCs (*1*, *2*), within the AGC Ser/Thr kinase superfamily. Distinct immune signaling themes have emerged for the PKCs, as reviewed by Tan and Parker (*3*), with roles implicated in immune modulatory responses, including key roles for PKCβ and PKCδ in B-cell tolerance, conventional PKCs signaling in mast cell degranulation, and the involvement of PKCε in macrophage function. PKCθ is highly expressed in T-cells, with some expression reported in mast cells, endothelial cells, and skeletal muscle (*4*−*8*). PKCθ plays a central role in T-cell receptor (TCR)-mediated signaling and is recruited to the supramolecular activation complex (*9*−*13*). PKCθ-deficient mice are viable, but mature T-cells are defective in proliferation and signaling to IL-2 production (*14*, *15*). The PKCθ-deficient mice show impaired

* To whom correspondence should be addressed. E-mail: dchaudhary@wyeth.com. Phone: (617) 665-5428. Fax: (617) 665-5419.

[‡] Department of Chemical and Screening Sciences.

[§] Department of Inflammation.

[||] Department of Protein Technologies.

[1] Abbreviations: AHR, airway hyperresponsiveness; Csk, C-terminal Src kinase; DTT, dithiothreitol; HEPES, *N*-(2-hydroxyethyl)piperazine-*N*′-2-ethanesulfonic acid; Il, interleukin; KD, kinase domain; PDK-1, 3-phosphoinositide-dependent protein kinase 1; pI, isoelectric point; PKA, protein kinase A; PKCθ, protein kinase C θ; TCR, T-cell receptor.

10.1021/bi050608q CCC: $30.25
Published on Web 06/24/2005

pulmonary inflammation and airway hyperresponsiveness (AHR) in a Th2-dependent murine asthma model, with no defects in viral clearance and Th1-dependent cytotoxic T-cell function (*16*, *17*). The impaired Th2 cell responses result in reduced levels of IL-4 and IgE, contributing to the AHR and inflammatory pathophysiology. No consequence on Th1 cell effector functions was observed, thus presenting PKCθ as a unique therapeutic target in Th2-mediated diseases.

PKCθ contains an N-terminal regulatory domain and a C-terminal catalytic kinase domain that is highly homologous to the catalytic domain of the other PKC kinases [Figure 1A (*18*)]. The regulatory domain contains the pseudosubstrate and cofactor binding motifs. The kinase domain contains the ATP and substrate binding sites that typically include conserved phosphorylation sites within the activation loop (Thr_{538}), a turn motif (Ser_{676}), and a hydrophobic motif (Ser_{695}). Phosphorylation of the highly conserved activation loop is required for enzymatic activity for PKC kinases (*18*). Kinase function is highly regulated posttranslationally, with protein phosphorylation being the key central modification in the different pathways and modulations. X-ray structure analysis of the PKCθ kinase domain indicates that all three oxygens of the conserved phosphate in phospho-Thr_{538} ($pThr_{538}$) are involved in hydrogen bonding interactions (*19*). The phosphoamino acid $pThr_{538}$ is located beneath helix αC and is proposed to compensate for the conserved cationic cluster formed by Arg_{503} and Lys_{527}, likely analogous to the interactions of $pThr_{197}$ with Arg_{165} and Lys_{189} in PKA, a close relative of the PKC family within the AGC kinase superfamily (*20*, *21*). These ionic interactions stabilize the correct orientation of the catalytic base Asp_{504} in PKCθ and Asp_{166} in PKA. Phosphorylated activation loop interactions further correctly position helix αC, bringing the DFG motif, and the catalytic Lys_{409} in PKCθ and Lys_{72} in PKA, within hydrogen bonding distance of the invariant Glu_{428} in PKCθ and Glu_{91} in PKA, respectively.

In addition to the interactions described above in the active site that regulate catalysis, activation loop phosphorylation may result in enhanced substrate access to the active site of the phosphorylated enzyme (*20*). This activation loop phosphorylation on conventional PKCs, novel PKCδ, and atypical PKCζ is carried out by another Ser/Thr kinase, PDK-1 (*22*−*26*), thereby generating a catalytically competent conformation that in turn autophosphorylates the hydrophobic and turn motifs. The activation mechanism of PKCθ has been hypothesized to involve activation loop phosphorylation by PDK-1 (*27*).

Although cofactor regulation that confers upon the subfamily distinction among the PKC isoforms has been described in the literature (*28*), the kinetic mechanisms and consequences of activation loop phosphorylation are not well understood. To date, kinetic analysis has been performed with only the conventional PKCs. Results from initial velocity studies with the catalytic domain of the rat PKCα and -β isoforms utilizing histone as the protein substrate were consistent with a sequential mechanism of substrate addition (*29*). Product and dead-end inhibition analysis of the rat PKCα and -γ isoforms further characterized the kinetic mechanism of the conventional PKCs as an ordered sequential mechanism with ATP binding first and ADP being released last (*30*). In these studies, the effect of cofactor and ionic strength upon catalysis was investigated, but there have

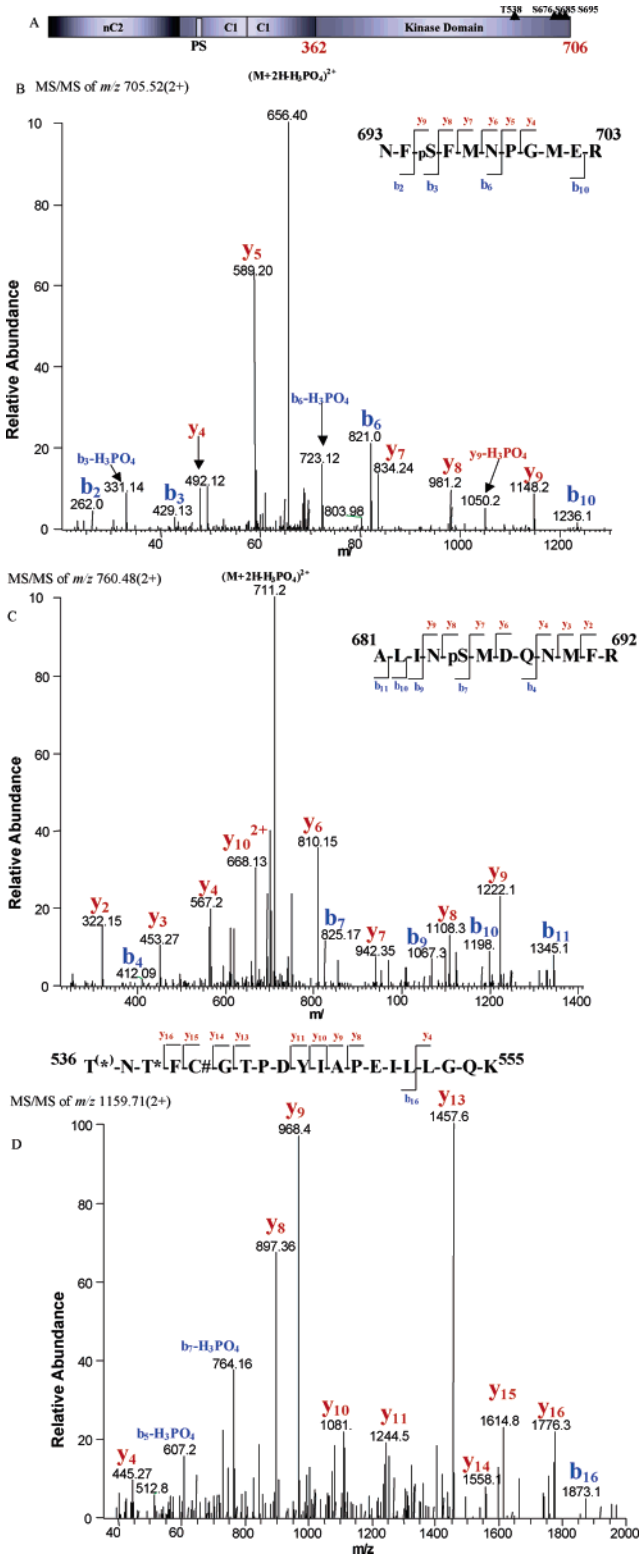

FIGURE 1: Characterization of PKCθ KD autophosphorylation. (A) PKCθ full-length schematic indicating the novel C2 domain, the cofactor binding C1 domains, and the kinase domain, with the conserved phosphorylation sites indicated in black. PKCθ KD N-terminal and C-terminal amino acid residues are labeled in red. Product ion spectra of (B) NFpSFMNPGMER at *m*/*z* 705.52, which indicates that Ser_{695} is the phosphorylation site, (C) ALINpSMDQNMFR at *m*/*z* 760.48, which indicates that Ser_{685} is the phosphorylation site, and (D) TNTFC#GTPDYIAPEILLGQK at *m*/*z* 1159.71, indicating one phosphate on this peptide. The product ion spectrum indicates that the phosphorylation site is either Thr_{536} or Thr_{538}. The cysteine alkylated by iodoacetamide is followed by #.

been no mechanistic studies to investigate the rate-limiting steps of PKC catalysis.

We undertook studies to elucidate the catalytic mechanism of the kinase domain of a novel PKC subfamily member, PKCθ. We characterized autophosphorylation of the PKCθ kinase domain (PKCθ KD) expressed in *Escherichia coli*, and the identified phosphorylation sites were subjected to mutation analysis to investigate effects on activation loop phosphorylation and function. A series of mechanistic experiments were performed to determine the catalytic constants and the rate-limiting steps of substrate phosphorylation. Dead-end and product inhibition experiments established the kinetic mechanism for PKCθ. The rate-limiting step of product release was established through viscosity studies and the nature of the phospho-transfer step by the use of ATP analogues. The results are indicative of a sequential ordered mechanism in which ATP binds first and ADP is released last. Our studies with the PKCθ KD provide the first mechanistic insight into the novel PKC kinase domain enzymatic function, and phosphorylation regulation unique to PKCθ.

MATERIALS AND METHODS

Expression and Purification of the Kinase Domain. The PKCθ KD, amino acid residues 362−706, was cloned into a pET16b expression vector, introducing a hexahistidine tag to the C-terminus, and used to transform *E. coli* strain BL21-DE3 for overexpression. A 10 L cell culture at 37 °C with an optical density of 0.4 was induced with 0.1 mM IPTG at 25 °C for 3 h prior to harvesting and resuspension in buffer [25 mM Tris (pH 8.0), 25 mM NaCl, 5 mM 2-mercaptoethanol, 5 mM imidazole, 50 μM ATP, and protease inhibitors] for lysis using a microfluidizer. The lysate was applied to 20 mL of nickel−NTA resin for 1 h at 4 °C. The resin was then poured as a chromatography column and washed extensively with the same buffer including 25 mM imidazole. Protein bound to the resin was eluted with 200 mM imidazole buffer. The protein was immediately loaded onto an HQ anion exchanger, and the column was washed with 25 mM Tris (pH 8.0), 25 mM NaCl, 5 mM DTT, and 50 μM ATP before being resolved by the application of a linear gradient from 25 to 500 mM NaCl. Fractions containing the PKCθ KD were selected by SDS−PAGE, pooled, diluted 2-fold with 25 mM Tris (pH 8.0) and 5 mM DTT, and loaded onto a heparin chromatography column. The flow through was immediately applied to a hydroxyapatite column and washed extensively with 25 mM Tris (pH 8.0), 50 mM NaCl, and 5 mM DTT. A linear gradient of sodium phosphate from 0 to 100 mM eluted the target protein. The protein was sized as a monomer by Superdex 200 size exclusion chromatography, dialyzed overnight at 4 °C against 25 mM Tris (pH 8.0), 50 mM NaCl, and 5 mM DTT, and concentrated.

Mass Spectrometric Analysis. The PKCθ KD [in 50 mM Hepes (pH 7.5), 5 mM $MgCl_2$, 5 mM DTT, 10% glycerol, and 0.0025% Brij-35 at 0.25 μg/μL] was run on 10% Tricine gels (Invitrogen) and stained with Comassie blue. The bands were excised and subjected to in-gel digestion with trypsin (Promega, Madison, WI) in a ProGest Investigator robot (Genomics Solutions, Ann Arbor, MI). The sample volume was reduced with a SpeedVac and reconstituted with 0.1 M acetic acid to a final volume of ~30 μL. The peptides were subjected to nanoLC−MS/MS analysis. Briefly, samples were injected onto a 75 μm × 10 cm IntegraFrit column (New Objectives, Woburn, MA) that was packed with 10 μm C18 beads (YMC, Wilmington, NC). The HPLC gradient increased linearly from 4 to 60% solvent B (solvent A, 0.1 M acetic acid and 1% ACN; solvent B, 0.1 M acetic acid and 90% ACN) over 45 min with a flow rate of 250 nL/min. Mass spectra were collected using a LCQ DECA XP ion trap mass spectrometer (ThermoFinnigan, San Jose, CA). The MS/MS data were searched against PKCθ for differential phosphorylation modification on serine, threonine, and tyrosine, using the Sequest algorithm (ThermoFinnigan).

Mutations, Immunoblotting, and Kinase Assays. The various constructs were generated by site-directed mutageneis (Stratagene) in the PKCθ KD expression construct and confirmed by sequencing. The constructs were expressed as described above, and equivalent amounts of *E. coli* lysates were analyzed by immunoblot and kinase assays after protein estimation by the Bradford assay (Bio-Rad). Briefly, lysates were analyzed by 4−20% SDS−PAGE, transferred to nitrocellulose, and immunoblotted with the indicated antibodies (anti-pT_{538} PKCθ from Cell Signaling Technologies and anti-His from Invitrogen) in a 5% blotto/0.05% TBS-Tween mixture. *E. coli* lysate kinase assays were performed with a final concentration of 83 μM biotinylated peptide substrate (FARKGSLFQ), 166 μM ATP, 0.5 μL of [^{33}P]ATP (specific activity of 3000 Ci/mmol or 10 mCi/mL), 84 ng/μL phosphatidylserine, 8.4 ng/μL diacylglycerol in 20 mM MOPS (pH 7.2), 25 mM β-glycerophosphate, 1 mM DTT, and 1 mM $CaCl_2$, in 30 μL for 30 min at room temperature. Five to ten microliters of the reaction mixture was spotted on phosphocellulose paper and then washed three times in 0.75% phosphoric acid and once in acetone. Scintillation cocktail was added to the phosphocellulose paper, and bound radioactivity was detected with a scintillation counter.

Enzyme Kinetics Assays. ATP, ATPγS, Ficoll-400, sucrose, ATP, ADP, phosphoenolpyruvate (PEP), NADH, pyruvate kinase (PK), lactate dehydrogenase (LDH), AMP-PNP, acetonitrile, and the buffer HEPES were purchased from Sigma Chemical Co. (St. Louis, MO). Peptide substrates, inhibitors, and phosphorylated substrate peptides were from AnaSpec (San Jose, CA), SynPep (Dublin, CA), or Open Biosystems (Huntsville, AL). The enzymatic activity was determined at 25 °C using the coupled PK/LDH assay, at 340 nm on a Molecular Devices plate reader. The standard reaction, except where indicated, was carried out in a final volume of 80 μL, in 25 mM HEPES (pH 7.5), 10 mM $MgCl_2$, 2 mM DTT, 0.008% Triton X-100, 100 mM NaCl, 20 units of PK, 30 units of LDH, 0.25 mM NADH, 2 mM PEP, and the PKCθ KD (0.156−0.312 μg/mL).

Solvent Viscosity Studies. Steady-state kinetic parameters were determined in the buffer described above containing varied sucrose (0−35%) or Ficoll-400 (0−8%) levels. Relative solvent viscosities (η^{rel}) were determined in triplicate relative to 25 mM HEPES (pH 7.5), 10 mM $MgCl_2$, 2 mM DTT, and 100 mM NaCl at 25 °C using an Ostwald viscometer. Buffer with no viscogen is indicated with a superscript 0. The coupling enzyme system was unaffected by the presence of these viscogens. Thio effect studies with ATPγS and product inhibition studies with ADP were analyzed on a Hewlett-Packard series 1100 HPLC system using a Phenomenex Auga 5 m C18 124 Å 50 mm × 4.60

mm column (00B-4299-E0). Phosphorylated peptide was separated from nonphosphorylated peptide using a gradient of 0 to 100% 20 mM phosphate (pH 8.8) and acetonitrile (50:50). The fluorescein-labeled peptide was detected by excitation at 485 nm and by monitoring the fluorescence emission at 530 nm.

Substrate Kinetics. Data were fitted to eq 1 for normal Michaelis−Menten kinetics or eq 2 for substrate inhibition:

$$v = \frac{V_{max}[S]}{K_m + [S]} \quad (1)$$

$$v = \frac{V_{max}[S]}{K_m + [S] + \frac{[S]^2}{K_i}} \quad (2)$$

where S is the substrate, V_{max} is the maximum enzyme velocity, K_m is the Michaelis constant, and K_i is the inhibition constant for substrate inhibition. The initial rates obtained at various fixed concentrations of peptides and ATP were fitted to the equations listed below:

$$v = \frac{V_{max}[A][B]}{K_{ia}K_b + K_b[A] + K_a[B] + [A][B]} \quad (3)$$

$$v = \frac{V_{max}[A][B]}{K_b[A] + K_a[B] + [A][B]} \quad (4)$$

In the above equations, [A] and [B] are ATP and peptide concentrations, respectively, K_a and K_b are the K_m values for ATP and peptide, respectively, and K_{ia} is the dissociation constant for the dissociation of A from the E−A complex.

Product and Dead-End Inhibition Kinetics. The initial reaction rates were obtained either as a function of product inhibition (ADP or phosphopeptide) or as a function of dead-end inhibition (AMP-PNP). In these studies, the concentration of one substrate is held constant while the other is varied against increasing concentrations of the inhibitor. In the case of product inhibition, the nonvaried substrate is held at saturating or nonsaturating levels, while in dead-end inhibition, the nonvaried substrate is held at saturating levels. The data were fit to a competitive inhibition model (eq 5), a noncompetitive inhibition model (eq 6), or an uncompetitive inhibition model (eq 7):

$$v = \frac{V_{max}[S]}{K_m\left(1 + \frac{[I]}{K_{is}}\right) + [S]} \quad (5)$$

$$v = \frac{V_{max}[S]}{K_m\left(1 + \frac{[I]}{K_{is}}\right) + [S]\left(1 + \frac{[I]}{K_{ii}}\right)} \quad (6)$$

$$v = \frac{V_{max}[S]}{K_m + [S]\left(1 + \frac{[I]}{K_{ii}}\right)} \quad (7)$$

where K_{ii} and K_{is} are the intercept and slope inhibition constants, respectively. The data were analyzed using Sigma Plot 2000 Enzyme Kinetics Module from SPSS Science (Richmond, CA).

RESULTS

Characterizaion of PKCθ KD Autophosphorylation. We expressed and purified the catalytically active PKCθ KD for analysis of the phosphorylation sites. A majority of the expressed protein in *E. coli* is in the insoluble fraction (data not shown), likely due to improper folding. However, the PKCθ KD that was highly active and stable was purified from the soluble fraction, enabling the structural characterization reported elsewhere (*19*) and the studies reported here. The PKCθ KD is phosphorylated as evidenced by mass spectrometry characterization. As PKCθ KD expression was carried out in *E. coli*, where there are no serine-threonine kinases, the mass spectrometry finding is a consequence of autophosphorylation by the expressed kinase. The predicted mass based on the amino acid sequence is 41 615 Da. However, the molecular mass determined by ESI-MS was 42 092 and 42 173 Da (50% each species), indicative of autophosphorylation of five or six amino acids in *E. coli*. Like the stable kinase activity, the phosphorylation state was stable and phosphatase inhibitors were not required in the expression purification scheme.

These experiments identified the hydrophobic motif Ser_{695} and the turn motif Ser_{685} as autophosphorylation sites (Figure 1B,C). Mass spectrometry did not detect any phosphorylation at Ser_{662} and Ser_{657} turn motif residues. On the basis of homologies with other PKC turn motifs, Ser_{676} was expected to be autophosphorylated, but this is not evident in these experiments as Ser_{676} was not detected in a tryptic peptide. These experiments further revealed that either Thr_{536} or Thr_{538} in the activation loop is also autophosphorylated (Figure 1D). X-ray structure determination of the bacterially expressed PKCθ KD confirmed the Thr_{538} residue is phosphorylated (*19*). This result is in contrast to the notion that the activation loop is phosphorylated by PDK-1 (*23*, *24*). Studies of kinase-dead full-length PKCθ mutant K409W by Liu et al. (*27*) have shown that this molecule is not phosphorylated at Thr_{538}. Using the HEK293 cell heterologous expression system, we also observed the lack of Thr_{538} phosphorylation of the K409W PKCθ mutant in cells (data not shown). This finding implies a lack of Thr_{538} phosphophorylation due to the K409W kinase mutant's inability to autophosphorylate. Furthermore, the K409W PKCθ molecule's abrogated Thr_{538} phosphorylation correlates with both a lack of in vitro cell lysate kinase activity and endogenous IKKα/β phosphorylation (data not shown).

Ser_{695} Is Required for Optimal Thr_{538} Autophosphorylation. It has been previously shown that amino acid residue Thr_{538} in the activation loop is required for kinase activity (*27*). Several phosphorylation site point mutations within the kinase domain were examined for their effects on activation loop Thr_{538} autophosphorylation (Figure 2). Soluble bacterial lysate fractions expressing the various phosphorylation site mutations were analyzed via a radioactive filter kinase assay and Western blot, because the mutations were not as amenable to purification. Thus, the kinase activity in the lysate fractions was correlated with the extent of Thr_{538} autophosphorylation in the corresponding fraction, to help establish the phosphorylation site mutagenesis correlations. Equivalent expression levels of the mutants in *E. coli* lysates

Table 1: Peptides Used in Assays with the PKCθ KD

peptide	sequence		source	pI
1	FARKGSLRQ	substrate	pseudosubstrate PKC α	12.01
2	RFARKGSLRQKNV	substrate	pseudosubstrate PKC α	12.31
3	LKRSLSEM	substrate	serum response factor	8.75
4	RTPKLARQASIELPSM	substrate	lymphocyte-specific protein 1	10.84
5	FARKGALRQ	inhibitor	pseudosubstrate PKC α	12.01

are shown in the anti-His Western blot panel. The autophosphorylation of Thr_{538} of the bacterially expressed PKCθ KD is further evidenced in the top panel of pThr$_{538}$-specific Western blot analysis. The lysate kinase activity consistently correlates with the extent of pThr$_{538}$ detected in the lysate for each of the expressed mutants, as shown in Figure 2. Ser_{695} in the C-terminal hydrophobic motif is required for optimal activation loop autophosphorylation, as evidenced by the significantly reduced signal in the anti-pThr$_{538}$ Western blot panel. Ser_{695} is obligatory for PKCθ KD kinase activity, as demonstrated by the lack of kinase activity, much like the inactive and kinase-dead mutations T538A and K409W, respectively (Figure 2). In contrast, turn motif residue Ser_{662} is dispensable for both activity and Thr_{538} autophosphorylation, while turn motif residues Ser_{676} and Ser_{685} have a partial impact.

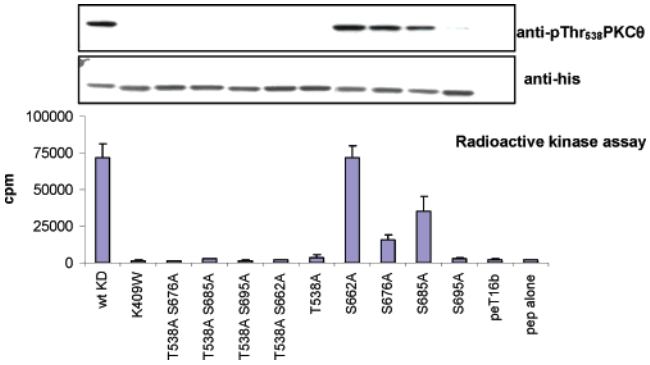

FIGURE 2: S695A attenuates PKCθ KD Thr_{538} autophosphorylation. *E. coli* lysates of the indicated PKCθ KD protein and mutations were assayed by Western blots for anti-pThr$_{538}$ PKCθ (top panel) followed by anti-His (bottom panel), confirming equivalent expression. Corresponding in vitro lysate kinase activity is depicted in the graph below.

Characterization of Steady-State Kinetic Constants of the PKCθ KD. Having established the phosphorylation site relationship of the expressed active PKCθ KD, we undertook detailed enzyme mechanism studies to examine the kinase catalytic reaction. The peptide substrates investigated for use in determining the kinetic mechanism of PKCθ are illustrated in Table 1. Peptide 1 and peptide 2 are substrates derived from the pseudosubstrate region of PKCα. Peptide 3 and peptide 4 are derived from the phosphorylation site in serum response factor (*31*) and the phosphorylation site in lymphocyte-specific protein-1, respectively (*32*). As shown in Table 2, in the absence of peptide substrate, the PKCθ KD hydrolyzed ATP 110 times slower (0.16 s^{-1}) than when peptide is present (18 s^{-1}). The K_m values for ATP of 59 μM (no peptide) and 49 μM (at saturating peptide 1 concentrations) show that there is no significant difference in the binding of ATP in the presence of the peptide substrate. The steady-state kinetic parameters for PKCθ at saturating ATP concentrations are listed in Table 2. Peptide 3 and peptide 4 show the highest K_m for PKCθ with values of 420 and 240 μM, respectively. In contrast, peptide 1 and peptide 2 have K_m values of 6.5 and 4.3 μM, respectively, and cause inhibition of the enzyme at high concentrations (Table 2). The lower K_m values of the more basic peptides 1 and 2 imply a basic amino acid substrate peptide preference for PKCθ.

Table 2: Summary of Steady-State Kinetic Parameters

varied substrate[a]	app K_m (μM)	k_{cat} (s^{-1})	$K_{i-peptide}$ (μM)	k_{cat}/K_m (M^{-1} s^{-1})	[NaCl] (mM)
peptide 1	6.5 ± 0.8	18 ± 1	>2000	2700000	100
peptide 2	4.3 ± 0.8	16 ± 1	306 ± 57	3600000	100
peptide 3	420 ± 21	21 ± 1		51000	100
peptide 4	240 ± 16	14 ± 1		58000	100
ATP	49 ± 5	18 ± 1		360000	50
ATP[b]	59 ± 8	0.16 ± 0.01		2600	50

[a] Peptides 1 and 2 fit to eq 2; peptides 3 and 4 and ATP fit to eq 1. [b] No peptide present in assay. The parameters used are defined as follows: app K_m, apparent Michaelis constant; k_{cat}, catalytic constant; $K_{i-peptide}$, substrate inhibition constant for peptide; k_{cat}/K_m, second-order rate constant.

Table 3: Effects of NaCl on PCKθ KD Steady-State Kinetic Parameters

[NaCl] (mM)	app K_{m-ATP}[a,b] (μM)	k_{cat}[b] (s^{-1})	app $K_{m-peptide\ 1}$[c] (μM)	$K_{i-peptide\ 1}$[c] (μM)
0	25 ± 5	7.5 ± 0.8	6.4 ± 4.2	129 ± 64
50	58 ± 8	18 ± 1	6.7 ± 2.8	20 ± 85
100	76 ± 7	22 ± 1	3.2 ± 1.0	>2000
250	121 ± 16	24 ± 1	9.0 ± 1.2	−

[a] At 0.2 mM peptide 1. [b] Fit to eq 1. [c] Fit to eq 2.

Ionic Strength Affects the PKCθ KD Catalysis. Interestingly, the substrate inhibition observed with the longer more basic peptide 2 was more pronounced than for the shorter peptide 1 (Table 2). Therefore, the kinetic parameters for PKCθ (peptide 1 and ATP) were examined at increasing NaCl concentrations (Table 3). As the concentration of NaCl is increased, both the K_m for ATP and the turnover rate of the enzyme increases, while the K_m for peptide 1 remains relatively constant. Ionic strength effects on PKCθ were also investigated by examining the effect of NaCl on substrate inhibition that occurs when the substrate combines with the enzyme in a nonproductive or dead-end complex. Substrate inhibition was observed for preferred basic peptides 1 and 2, but not observed for less optimal peptides 3 and 4 (Table 2). Furthermore, substrate inhibition was also found to be dependent on the ionic strength of the buffer. Substrate inhibition with peptide 1 diminishes as the NaCl concentration is increased to 250 mM (Table 3).

PKCθ KD Initial Velocity Kinetics. In the determination of the kinetic mechanism of PKCθ, the initial velocity of the reaction with varied ATP concentrations was determined against fixed varied concentrations of the peptide substrate at 100 mM NaCl. The assay was first carried out with peptide

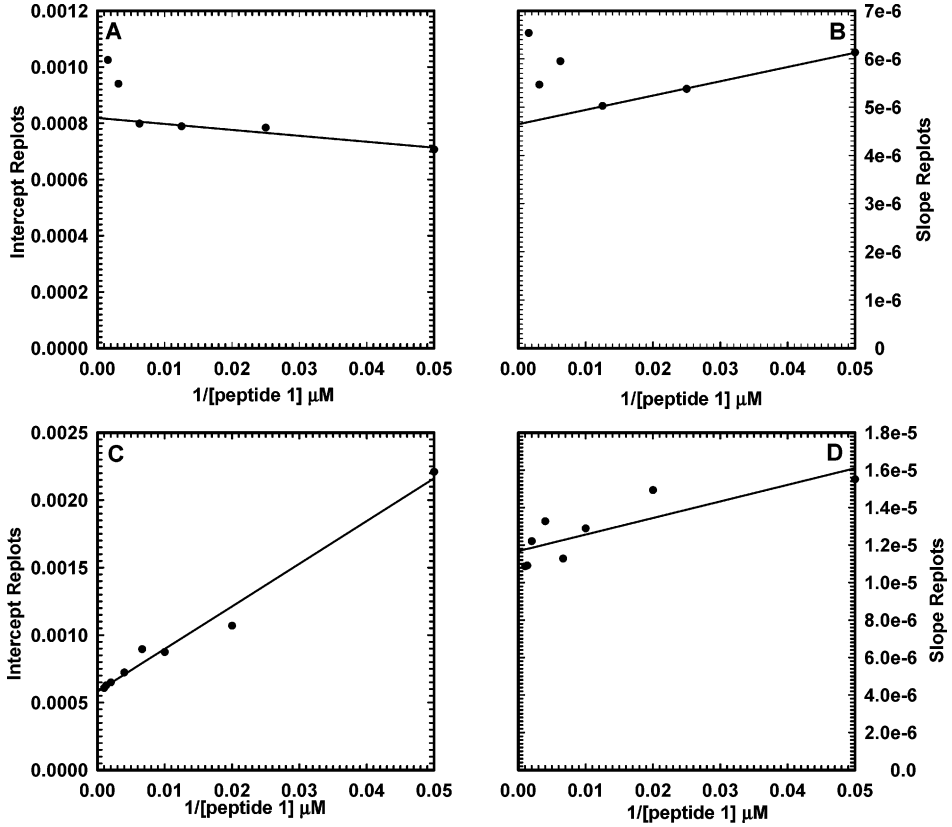

FIGURE 3: Substrate inhibition of peptide 1 by formation of the dead-end complex. At 100 mM NaCl: (A) intercept replot vs 1/[peptide 1] and (B) slope replot vs 1/[peptide 1]. At 625 mM NaCl: (C) intercept replot vs 1/[peptide 1] and (D) slope replot vs 1/[peptide 1].

1; however, the resulting Lineweaver−Burk plot was difficult to interpret due to peptide 1 substrate inhibition (data not shown). Intercept and slope replots against peptide 1 were nonlinear, as shown in panels A and B of Figure 3. The initial velocity assays were also performed using peptide 3 under identical conditions. Varied ATP concentrations versus fixed varied peptide 3 concentrations resulted in an intersecting pattern on a Lineweaver−Burk plot (data not shown) that indicates a sequential kinetic mechanism. The K_{ia} value for ATP was 61 ± 22 μM, and the K_a for ATP was 118 ± 17 μM. The initial velocity pattern with peptide 1 was then determined at 625 mM NaCl, as the increased salt concentration slows the substrate inhibition for peptide 1 (Table 3). The resulting Lineweaver−Burk plot produced an intersecting pattern as well (data not shown), consistent with a sequential kinetic mechanism when peptide 1 is the substrate. At high NaCl concentrations, intercept and slope replots against peptide 1 were linear (Figure 3C,D). The K_{ia} value for ATP of 66 ± 32 μM obtained at high NaCl concentrations is similar to the K_{ia} value for ATP of 61 ± 22 μM with peptide 3 at 100 mM NaCl. This indicates that the increased ionic strength did not affect the dissociation constant for dissociation of ATP from the enzyme−ATP complex. The K_a of ATP obtained at 625 mM NaCl was 321 ± 19 μM, in contrast to the K_a of ATP at 100 mM NaCl of 118 ± 17 μM. This is consistent with an increase in K_m for ATP as the ionic strength is increased (Table 3).

Dead-End Inhibition Studies Identify ATP as the First Substrate To Bind the PKCθ KD. We next sought to determine the substrate binding order in the sequential catalytic mechanism. AMP-PNP, a nonhydrolyzable analogue of ATP, and peptide 5, with a serine to alanine change from peptide 1 (Table 1), were used for inhibition studies. AMP-PNP was shown to be a competitive inhibitor of ATP with a K_i value of 228 μM (Table 4). There was no observed inhibition with AMP-PNP versus peptide, at saturating ATP concentrations. The peptide inhibitor, peptide 5, was shown to be a competitive inhibitor with respect to peptide 1 and peptide 3 with K_{is} values of 10 and 4.4 μM, respectively (Table 4). Peptide 5 was further shown to be an uncompetitive inhibitor against ATP with K_{ii} values of 1100 μM (Table 4). These results are consistent with an ordered sequential addition of substrates for PKCθ where ATP associates first with enzyme followed by peptide.

Product Inhibition Kinetics Identify ADP as the Last Product Released. Because the PK/LDH coupled kinase assay consumes the catalytic product ADP, an HPLC assay was used to determine the inhibition patterns with ADP (Table 4). ADP was found to be a competitive inhibitor against ATP at saturating peptide 1 concentrations with a K_{is} of 291 μM. No inhibition was observed when ADP was assayed against peptide 1, at saturating ATP concentrations. When the assay was performed at nonsaturating ATP concentrations (0.1 mM), a noncompetitive pattern was observed with a K_{is} of 494 μM and a K_{ii} of 200 μM (Table 4). These results with ADP rule out a random mechanism (Scheme 1C) but are consistent with either a sequential ordered (Scheme 1A) or Theorell−Chance (Scheme 1B) kinetic mechanism, wherein ADP is the final product that is released. To further elucidate the kinetic mechanism, product inhibition assays with phosphopeptide 1 were performed. Due to the substrate inhibition observed with peptide 1, the product inhibition assays were carried out with peptide 3. Phosphopeptide 1 was a noncompetitive inhibitor of peptide

Table 4: Inhibition Patterns and Constants[a]

inhibitor	type	substrate	pattern[b]	K_{is}[g] (μM)	K_{ii}[g] (μM)	equation[c]
ADP	product	ATP	c	291 ± 24		5
ADP	product	peptide 1	−			
ADP	product	peptide 1[d]	nc	494 ± 72	200 ± 29	6
phosphopeptide 1	product	ATP[e]	uc		1600 ± 100	7
phosphopeptide 1	product	peptide 3[f]	nc	1700 ± 1100	1200 ± 800	6
phosphopeptide 1	product	peptide 3[d,f]	uc		2000 ± 400	7
AMP-PNP	dead-end	ATP	c	228 ± 29		5
AMP-PNP	dead-end	peptide 1	−			
peptide 5	dead-end	peptide 1	c	10 ± 3		5
peptide 5	dead-end	ATP	uc		1100 ± 100	7
peptide 5	dead-end	peptide 3	c	4.4 ± 0.3		5

[a] NaCl concentration held at 100 mM. [b] c, competitive; nc, noncompetitive; uc, uncompetitive; −, no inhibition observed. [c] Data fit to this equation. [d] ATP concentration held at 0.1 mM. [e] Peptide 3 concentration held at 0.5 mM; peptide 3 used because of the low K_m of peptide 1. [f] Peptide 3 used due to substrate inhibition observed with peptide 1. [g] K_{is}, inhibition constant slope effect; K_{ii}, inhibition constant intercept effect.

Scheme 1: Sequential Binding Mechanisms[a]

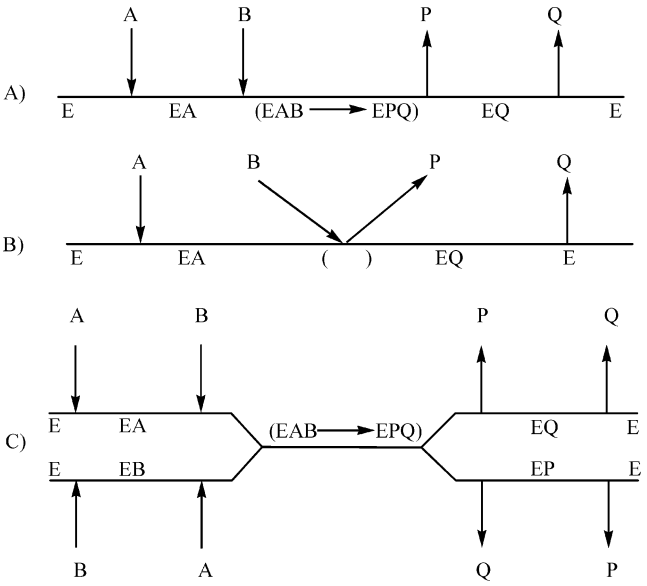

[a] E is the enzyme, A the peptide, B ATP, P the phosphopeptide, and Q ADP.

3, with a K_{is} of 1700 μM and a K_{ii} of 1200 μM, at a saturating ATP concentration (Table 4). At nonsaturating ATP concentrations, an uncompetitive pattern was observed, with a K_{ii} of 2000 μM. Phosphopeptide 1 was an uncompetitive inhibitor against ATP, at a nonsaturating peptide 3 concentration (0.5 mM), with a K_{ii} of 1600 μM. The results described above are more consistent with a sequential ordered bi-bi mechanism, with ADP as the last product released (Scheme 1A).

Phospho Transfer and Product Release Contribute to the Catalytic Rate-Limiting Steps. The rate of the phosphotransfer step in the catalysis was investigated using the thio analogue of ATP, ATPγS. Substitution of ATPγS for ATP resulted in a large change in the k_{cat} of the reaction (Table 5). The ATPγS reaction compared to the reaction with ATP is 112- and 146-fold slower in 100 and 250 mM NaCl, respectively. However, the K_m for ATP and ATPγS obtained using HPLC differed by only 2-fold (Table 5). To determine if the chemical step is the lone contributor to the rate of the reaction, the effect of solvent viscosity on the steady-state kinetic parameters for PKCθ was determined. Two types of viscogens were employed in this study, the microviscogen

Table 5: Thio Effect upon the PKCθ KD

	[NaCl] (mM)	ATP[a]	ATPγS[a]	ATP:ATPγS ratio
app K_m (μM)	100	251 ± 24	120 ± 9	2.1
app K_m (μM)	250	234 ± 19	130 ± 5	1.8
rate[b]	100	179 ± 5	1.6 ± 0.1	112
rate[b]	250	190 ± 4	1.3 ± 0.1	146

[a] Peptide 1 used in the assay. [b] Rate equals peak area/(reaction time in minutes)(enzyme concentration in nanomolar).

sucrose and the macroviscogen Ficoll-400. Microviscogens directly affect the diffusion of small molecules while at the same time cause the viscosity effect observed with a viscometer (*33*). Macroviscogens cause viscosity effects seen with a viscometer but do not significantly affect the diffusion rate of the small molecules, thereby serving as a control for the microviscosity effect observed in the assay (*34*). The steady-state kinetic parameters of peptide 1, peptide 3, and ATP were determined at increasing solvent viscosities and at two different ionic strengths. The relative effects of solvent viscosity on the kinetic parameters, k_{cat} and k_{cat}/K_m, were plotted against the relative viscosity of the buffer and fit to a linear regression (Figure 4). A slope of 1 indicates a maximal effect of the microviscogen on the kinetic parameter. There was little effect on the enzymatic rate in the presence of the macroviscogen. As the microviscosity of the solvent increased, there was a moderate effect seen on the $(k_{cat})^{\eta}$ value. This was seen as a linear decrease in the observed rate of the enzyme with all three substrates studied at 100 and 250 mM NaCl. The slope $[(k_{cat})^{\eta}]$ obtained under all the conditions varied from 0.38 to 0.54, implying that product release is partially rate limiting (Figure 4A,C). A value of 0.8−1 indicates that product release is the catalytic rate-limiting step (*20*).

The stickiness of a substrate can be determined by viscosity analysis. Briefly, for a sticky substrate, the rate of product formation is faster than the rate of substrate dissociation, while a nonsticky substrate will dissociate from the enzyme at a rate faster than the rate of product formation (*35*). The relative effect of increased solvent microviscosity on k_{cat}/K_m is plotted against relative solvent viscosity (Figure 4B,D). When the effect of microviscosity was plotted against relative solvent viscosity for peptide 1, the slope had a $(k_{cat}/K_m)^{\eta}$ value of 0.86 in 250 mM NaCl (data not shown). Data were not obtained at 100 mM NaCl for peptide 1 due to the substrate inhibition observed at low ionic strengths. Peptide 3, on the other hand, showed no solvent viscosity effect at

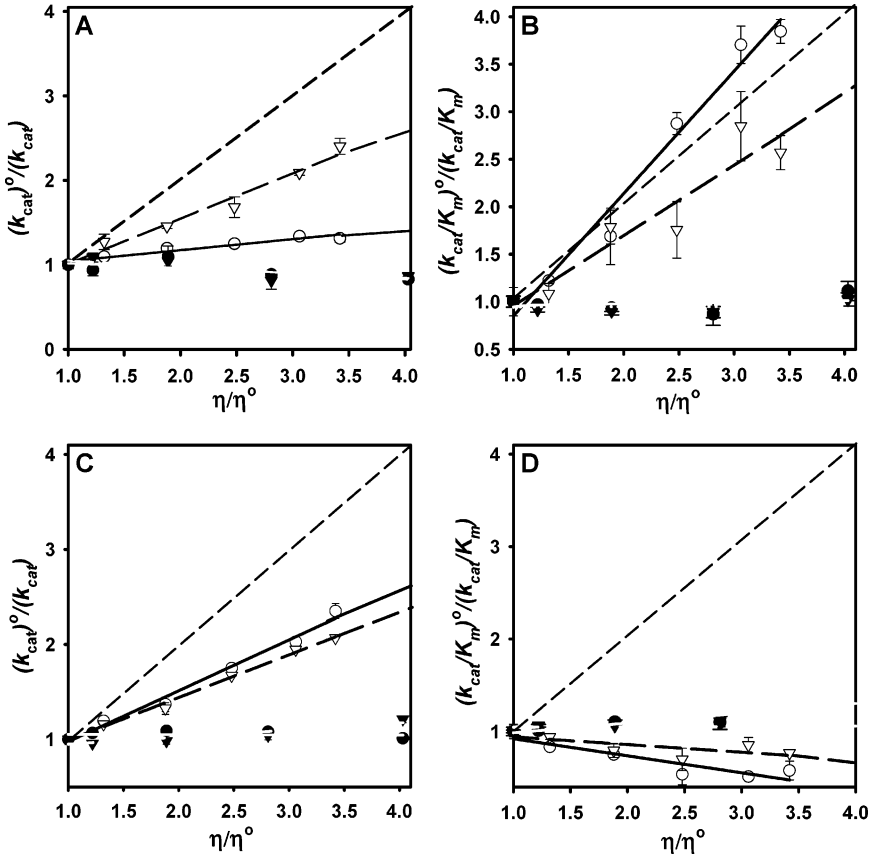

FIGURE 4: Solvent viscosity effects on k_{cat} and k_{cat}/K_m for the PKCθ KD. (A) k_{cat} effect with a varied peptide 1 concentration with the ATP concentration held at 2.0 mM. (B) k_{cat}/K_m for ATP at 0.125 mM peptide 1. (C) k_{cat} effect with a varied peptide 3 concentration with the ATP concentration held at 2.0 mM. (D) k_{cat}/K_m for peptide 3 at 2.0 mM ATP: (○) 100 mM NaCl, (▽) 250 mM NaCl in increasing sucrose concentrations, (●) 100 mM NaCl, and (▼) 250 mM NaCl in increasing Ficoll-400 concentrations. The dashed line indicates a slope of 1.

either ionic strength (Figure 4D). These studies imply that peptide 1 is a sticky substrate while peptide 3 is not sticky.

DISCUSSION

PKCθ KD Activation Loop Autophosphorylation. The bacterially expressed PKCθ KD is autophosphorylated at five or six amino acid residues on the basis of the mass spectrometry data. The phosphorylation sites identified in these experiments include hydrophobic motif Ser_{695}, turn motif Ser_{685}, and activation loop Thr_{538} or Thr_{536}. Ser_{685} is a newly identified autophosphorylation site in the turn motif. Turn motif Ser_{676} was not detected in a tryptic peptide, though Ser_{676} is predicted to be phosphorylated on the basis of sequence homology. Finally, in addition to the above-identified phosphorylation sites, at least two additional amino acid residues are autophosphorylated but not detected by these techniques.

Mass spectrometry analysis indicates that either Thr_{536} or Thr_{538} of the bacterially expressed PKCθ KD activation loop is autophosphorylated (Figure 1B−D). The identity of the phosphorylated residue is obtained from the X-ray structure, which revealed phosphorylated Thr_{538} in hydrogen bond interactions with the side chain of the preceding Thr_{536} (*19*). This interaction likely further stabilizes the interactions within the activation loop and with helix αC, both of which have relevance in catalysis (*36*). Previous studies have suggested a catalytic competent conformation for PKCθ wherein the activation loop is constitutively phosphorylated (*18*). PDK-1 phosphorylates PKCs and other AGC family kinases at the kinase domain activation loop, as a required modification that precedes autophosphorylation occurring at conserved sites on the hydrophobic and turn motifs (*18*, *23*). It has been previously suggested that while the hydrophobic and turn motifs are autophosphorylated, the PKCθ activation loop is phosphorylated by PDK-1 (*23*, *24*). Our results reveal that in contrast to bacterially expressed PKCζ (*37*), the PKCθ KD is uniquely capable of activation loop autophosphorylation and, therefore, does not have an obligatory PDK-1 phosphorylation requirement. In our characterization, we present evidence to support the premise that activation loop autophosphorylation occurs in addition to that of the hydrophobic and turn motifs in the PKCθ KD (Figure 1). These studies do not rule out the possibility that in cells PDK-1 can phosphorylate the full-length PKCθ activation loop.

PKCθ KD Regulation by the Hydrophobic and Turn Motif. Mutation analysis demonstrates that both Ser_{676} and Ser_{685} in the conserved turn motif partially impact the kinase function of the PKCθ KD (Figure 2). It has been reported previously that the S676A mutation in the full-length kinase does not affect kinase activity, while the S695A mutation in the full-length molecule reduced kinase activity by 80% (*27*). The residual activity of the S695A mutation reported in full-length PKCθ is consistent with a modest phospho-Thr_{538} signal observed here for the S695A mutation in the kinase domain construct context (Figure 2). This suggests that the Ser_{695} mutation results in a loss of optimal Thr_{538} autophosphorylation, consequently resulting in attenuation of kinase

activity. This feature is also unique to PKCθ among other PKC isoforms. In the case of PKCθ, it is likely that Ser_{695} autophosphorylation and Thr_{538} autophosphorylation are somewhat interdependent. A PKC molecule phosphorylated at the activation loop has been described as a "catalytic competent conformation" existing prior to cofactor binding, autophosphorylation, and substrate catalysis steps (*18*). For optimal PKCθ KD kinase function, it is likely that autophosphorylation of both the activation loop and hydrophobic motif contributes to this catalytic competent conformation.

Effect of Ionic Interactions on PKCθ Kinase Catalysis. Increases in buffer NaCl concentration increased the PKCθ KD K_m for ATP and accelerated enzyme turnover (Table 3). An ionic strength effect was also observed on peptide 1 substrate inhibition. As the NaCl concentration was increased, the extent of substrate inhibition observed with peptide 1 diminished (Table 3). The nature of the salt (NaCl) and its effect on ion-pair formation can provide insight into these observations. According to the Hofmeister series of cations and anions, NaCl falls in the midpoint of kosmotropes and chaotropes (*38*). Therefore, NaCl should not salt out the enzyme or denature the enzyme. However, increases in the ionic strength of the buffer would have an effect on the formation of ion pairs (*39*). With the tyrosine kinase Csk, the addition of 50 mM NaCl had the effect of increasing the K_m for the substrate poly(Gly,Tyr), a negatively charged substrate. However, there was no effect on the K_m for ATP or the turnover of the enzyme (*34*). In the case of the PKCθ KD, the increase in K_m for ATP may be a result of two possibilities. (1) At 250 mM NaCl, there is more productive binding of peptide 1 to the enzyme−ATP binary complex, and the observed K_m is a reflection of the actual K_m for ATP, or (2) the increase in ionic strength effects ATP, a charged substrate, in the same manner as peptide 1. It is possible that the observed increase in K_m is a result of a combination of the above two possibilities. With the peptide 1 substrate, ion-pair formation (Coulombic interactions) may be important in the binding of this substrate to the enzyme. At pH 7.5, a basic peptide such as peptide 1 would have a net positive charge. Therefore, increasing the NaCl concentration would result in a less favorable environment for ion-pair formation (*39*). If ion-pair formation contributes to the inhibition of peptide 1, then a decreasing level of substrate inhibition with an increasing NaCl concentration is consistent with weakening of the Columbic interactions.

PKCθ KD Kinetic Mechanism. The kinetic mechanisms for several kinases have been reported. Examples include a rapid equilibrium random mechanism for p21-activated kinase (*40*), a random mechanism for Rho-kinase II (*41*), and a sequential ordered mechanism for p38 MAP kinase (*42*, *43*). The mechanism of p38 MAP kinase was unique in that when a protein was the phosphate acceptor the protein substrate was the first to bind (*43*) whereas when a peptide was the phosphate acceptor ATP was the first to bind (*42*). PKCθ KD initial velocity plots, with both peptide substrates at high and low ionic strengths, resulted in graphs with lines intersecting left and below the ordinate. The pattern is a clear indication of a sequential mechanism that remained unaffected by the buffer ionic strength. In addition, there was no difference in the ATP K_{ia} values, 61 μM for peptide 3 at 100 mM NaCl and 66 μM for peptide 1 at 625 mM NaCl, further indicating that dissociation of ATP from the enzyme−ATP complex was not affected by the ionic strength. Under both conditions, the K_{ia} value is less than the K_a values of 118 and 321 μM, respectively, ruling out a rapid equilibrium mechanism.

Scheme 2: Substrate Inhibition Mechanisms[a]

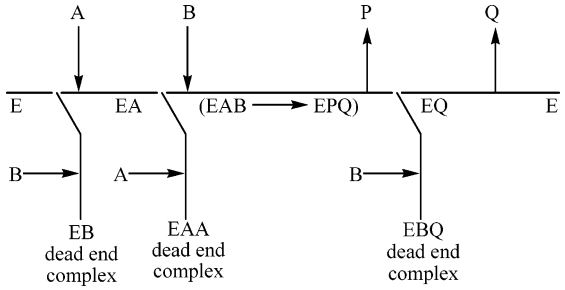

[a] E is the enzyme, A the peptide, B ATP, P the phosphopeptide, and Q ADP.

Dead-end inhibition and product inhibition studies (Table 4) are consistent with a sequential ordered mechanism, wherein ATP is the first substrate to bind. The peptide inhibitor (peptide 5 in Table 1) is competitive against both peptide substrates and uncompetitive against ATP. While the ATP analogue AMP-PNP is competitive against ATP, there is no observed inhibition against peptide 1 up to 2.0 mM AMP-PNP at saturating ATP concentrations. A competitive pattern is observed when the ATP concentration is varied against ADP concentration, and there is no inhibition observed when peptide 1 is varied against ADP concentration at saturating ATP concentrations. A noncompetitive pattern is observed when peptide 1 is varied against ADP concentration at nonsaturating ATP concentrations. These inhibition studies rule out a random mechanism for the PKCθ KD and demonstrate that ADP is the last product released as shown in Scheme 1A.

The initial velocity experiments at 100 mM NaCl with peptide 1 give some insight into the type of substrate inhibition observed. Briefly, there are three types of substrate inhibition observed in an ordered bireactant system (*44*) shown in Scheme 2. Two are substrate inhibition in which substrate B forms a dead-end E−B complex or substrate A forms a E−A−A dead-end complex. The third is substrate inhibition in which B forms an E−B−Q dead-end complex. The formation of the E−A−A dead-end complex is ruled out because the first substrate to associate is ATP and no substrate inhibition is observed with ATP. Figure 3 shows the replots of the initial velocity data at 100 and 625 mM NaCl for peptide 1. The effect of the inhibition is seen on both the slope and intercept replots at 100 mM NaCl (i.e., replots are not linear). However, at 625 mM NaCl, the replots become linear, indicating that the inhibition is abolished at high ionic strengths up to 0.5 mM peptide 1. The effect of substrate inhibition on both the slope and intercept replots is consistent with noncompetitive substrate inhibition (*45*). Noncompetitive substrate inhibition in an ordered sequential mechanism suggests the formation of the following types of nonproductive enzyme complexes. Two are represented in Scheme 2, the E−B complex and E−B−Q complex. A third possibility would be a nonproductive E−A−B complex. This is a distinct possibility because at 0 mM NaCl the substrate inhibition is potent (0.129 mM) and the ATP concentration is ~80K_m (0.025 mM at 0 mM NaCl). In a sequential ordered

mechanism in which ATP binds first, there would be little free enzyme present to form the E−B dead-end complex.

Effects of Viscosity and ATPγS on PKCθ KD Catalysis. Phosphorothioates are used to study different types of enzymatic phospho-transfer reactions. The ATPγS reaction occurred 15−20-fold slower than the ATP reaction in the case of Csk kinase (*34*). Similarly, in the enzymatic mechanism studies of phosphatidylinositol-specific phospholipase C (PLC), the reaction was slowed 10^5-fold when the nonbridging oxygen was substituted with sulfur (*46*). Regardless of which ATP analogue is used, ATP or ATPγS, the product, ADP, is identical. Thus, the catalytic rate will remain unaffected by product release. The thio effect observed for the PKCθ KD implies a contribution of the phospho-transfer chemistry to the overall rate of the enzymatic reaction. In addition, the large thio effect observed with PKCθ argues against a Theorell−Chance ordered sequential kinetic mechanism depicted in Scheme 1C (*47*). With a Theorell−Chance kinetic mechanism, the ternary complex is short-lived, therefore implying the chemical step is very fast.

The effect of solvent viscosity is a valuable tool in the determination of the rate-limiting step in an enzymatic reaction. The effect of increased solvent viscosity is seen on the nonchemical steps such as diffusion of the product from the enzyme and the diffusion of substrates to the enzyme active site, (*33*) and not on a unimolecular step such as the phospho-transfer step (*20*). The PKCθ solvent viscosity effect studies reported here indicate product release is a partly rate limiting step in the catalysis.

The studies presented here illustrate PKC enzyme catalysis characteristics and the kinetic mechanism, thereby providing insights into PKC isoforms and/or AGC family kinases that are highly similar to PKC. The results are consistent with a sequential ordered mechanism in which ATP binds first and ADP is released last. Phosphopeptide release and phospho transfer contribute to the rate-limiting steps. Importantly, features potentially unique to PKCθ are revealed in the phosphorylation studies of the kinase domain presented here. Taken together with the structural characteristics reported elsewhere (*19*), our findings have significant implications in advancing the selective targeting of this kinase for disease therapies and lay the groundwork for further mechanistic study of PKCθ.

REFERENCES

1. Baier, G., Telford, D., Giampa, L., Coggeshall, K. M., Baier-Bitterlich, G., Isakov, N., and Altman, A. (1993) Molecular cloning and characterization of PKC θ, a novel member of the protein kinase C (PKC) gene family expressed predominantly in hematopoietic cells, *J. Biol. Chem. 268*, 4997−5004.
2. Chang, J. D., Xu, Y., Raychowdhury, M. K., and Ware, J. A. (1993) Molecular cloning and expression of a cDNA encoding a novel isoenzyme of protein kinase C (nPKC). A new member of the nPKC family expressed in skeletal muscle, megakaryoblastic cells, and platelets, *J. Biol. Chem. 268*, 14208−14214; *269* (49), 31322 (Erratum).
3. Tan, S. L., and Parker, P. J. (2003) Emerging and diverse roles of protein kinase C in immune cell signalling, *Biochem. J. 376*, 545−552.
4. Mischak, H., Goodnight, J., Henderson, D. W., Osada, S., Ohno, S., and Mushinski, J. F. (1993) Unique expression pattern of protein kinase C-theta: High mRNA levels in normal mouse testes and in T-lymphocytic cells and neoplasms, *FEBS Lett. 326*, 51−55.
5. Baier, G., Baier-Bitterlich, G., Meller, N., Coggeshall, K. M., Giampa, L., Telford, D., Isakov, N., and Altman, A. (1994) Expression and biochemical characterization of human protein kinase C-θ, *Eur. J. Biochem. 225*, 195−203.
6. Mattila, P., Majuri, M. L., Tiisala, S., and Renkonen, R. (1994) Expression of six protein kinase C isotypes in endothelial cells, *Life Sci. 55*, 1253−1260.
7. Yamada, K., Avignon, A., Standaert, M. L., Cooper, D. R., Spencer, B., and Farese, R. V. (1995) Effects of insulin on the translocation of protein kinase C-θ and other protein kinase C isoforms in rat skeletal muscles, *Biochem. J. 308*, 177−180.
8. Liu, Y., Graham, C., Parravicini, V., Brown, M. J., Rivera, J., and Shaw, S. (2001) Protein kinase C θ is expressed in mast cells and is functionally involved in Fcε receptor I signaling, *J. Leukocyte Biol. 69*, 831−840.
9. Bi, K., Tanaka, Y., Coudronniere, N., Sugie, K., Hong, S., van Stipdonk, M. J., and Altman, A. (2001) Antigen-induced translocation of PKC-θ to membrane rafts is required for T cell activation, *Nat. Immunol. 2*, 556−563.
10. Bi, K., and Altman, A. (2001) Membrane lipid microdomains and the role of PKCθ in T cell activation, *Semin. Immunol. 13*, 139−146.
11. Das, V., Nal, B., Roumier, A., Meas-Yedid, V., Zimmer, C., Olivo-Marin, J. C., Roux, P., Ferrier, P., Dautry-Varsat, A., and Alcover, A. (2002) Membrane-cytoskeleton interactions during the formation of the immunological synapse and subsequent T-cell activation, *Immunol. Rev. 189*, 123−135.
12. Huang, J., Lo, P. F., Zal, T., Gascoigne, N. R., Smith, B. A., Levin, S. D., and Grey, H. M. (2002) CD28 plays a critical role in the segregation of PKC θ within the immunologic synapse, *Proc. Natl. Acad. Sci. U.S.A. 99*, 9369−9373.
13. Altman, A., and Villalba, M. (2003) Protein kinase C-θ (PKCθ): It's all about location, location, location, *Immunol. Rev. 192*, 53−63.
14. Sun, Z., Arendt, C. W., Ellmeier, W., Schaeffer, E. M., Sunshine, M. J., Gandhi, L., Annes, J., Petrzilka, D., Kupfer, A., Schwartzberg, P. L., and Littman, D. R. (2000) PKC-θ is required for TCR-induced NF-κB activation in mature but not immature T lymphocytes, *Nature 404*, 402−407.
15. Pfeifhofer, C., Kofler, K., Gruber, T., Tabrizi, N. G., Lutz, C., Maly, K., Leitges, M., and Baier, G. (2003) Protein kinase C θ affects Ca^{2+} mobilization and NFAT cell activation in primary mouse T cells, *J. Exp. Med. 197*, 1525−1535; *198* (1), 183 (Erratum).
16. Berg-Brown, N. N., Gronski, M. A., Jones, R. G., Elford, A. R., Deenick, E. K., Odermatt, B., Littman, D. R., and Ohashi, P. S. (2004) PKCθ signals activation versus tolerance in vivo, *J. Exp. Med. 199*, 743−752.
17. Marsland, B. J., Soos, T. J., Spath, G., Littman, D. R., and Kopf, M. (2004) Protein kinase C θ is critical for the development of in vivo T helper (Th)2 cell but not Th1 cell responses, *J. Exp. Med. 200*, 181−189.
18. Newton, A. C. (2003) Regulation of the ABC kinases by phosphorylation: Protein kinase C as a paradigm, *Biochem. J. 370*, 361−371.
19. Xu, Z. B., Chaudhary, D., Olland, S., Wolfrom, S., Czerwinski, R., Malakian, K., Lin, L., Stahl, M. L., Joseph-McCarthy, D., Benander, C., Fitz, L., Greco, R., Somers, W. S., and Mosyak, L. (2004) Catalytic domain crystal structure of protein kinase C-θ (PKCθ), *J. Biol. Chem. 278*, 50401−50409.
20. Adams, J. A. (2003) Activation loop phosphorylation and catalysis in protein kinases: Is there functional evidence for the autoinhibitor model, *Biochemistry 42*, 601−607.
21. Huse, M., and Kuriyan, J. (2002) The conformational plasticity of protein kinases, *Cell 109*, 275−282.
22. Hodgkinson, C. P., and Sale, G. J. (2002) Regulation of both PDK1 and the phosphorylation of PKC-ζ and -δ by a C-terminal PRK2 fragment, *Biochemistry 41*, 561−569.
23. Balendran, A., Hare, G. R., Kieloch, A., Williams, M. R., and Alessi, D. R. (2000) Further evidence that 3-phosphoinositide-dependent protein kinase-1 (PDK1) is required for the stability and phosphorylation of protein kinase C (PKC) isoforms, *FEBS Lett. 484*, 217−223.
24. Le Good, J. A., Ziegler, W. H., Parekh, D. B., Alessi, D. R., Cohen, P., and Parker, P. J. (1998) Protein kinase C isotypes controlled by phosphoinositide 3-kinase through the protein kinase PDK1, *Science 281*, 2042−2045.
25. Sonnenburg, E. D., Gao, T., and Newton, A. C. (2001) The phosphoinositide-dependent kinase, PDK-1, phosphorylates con-

ventional protein kinase C isozymes by a mechanism that is independent of phosphoinositide 3-kinase, *J. Biol. Chem. 276*, 45289−45297.
26. Cenni, V., Doppler, H., Sonnenburg, E. D., Maraldi, N., Newton, A. C., and Toker, A. (2002) Regulation of novel protein kinase C ϵ by phosphorylation, *Biochem. J. 363*, 537−545.
27. Liu, Y., Graham, C., Li, A., Fisher, R. J., and Shaw, S. (2002) Phosphorylation of the protein kinase C-θ activation loop and hydrophobic motif regulates its kinase activity, but only activation loop phosphorylation is critical to in vivo nuclear-factor-κB induction, *Biochem. J. 361*, 255−265.
28. Newton, A. C. (2001) Protein kinase C: Structural and spatial regulation by phosphorylation, cofactors, and macromolecular interactions, *Chem. Rev. 101*, 2353−2364.
29. Hannun, Y. A., and Bell, R. M. (1990) Rat brain protein kinase C. Kinetic analysis of substrate dependence, allosteric regulation, and autophosphorylation, *J. Biol. Chem. 265*, 2962−2972.
30. Leventhal, P. S., and Bertics, P. J. (1991) Kinetic analysis of protein kinase C: Product and dead-end inhibition studies using ADP, poly(L-lysine), nonhydrolyzable ATP analogues, and diadenosine oligophosphates, *Biochemistry 30*, 1385−1390.
31. Heidenreich, O., Neininger, A., Schratt, G., Zinck, R., Cahill, M. A., Engel, K., Kotlyarov, A., Kraft, R., Kostka, S., Gaestel, M., and Nordheim, A. (1999) MAPKAP kinase 2 phosphorylates serum response factor in vitro and in vivo, *J. Biol. Chem. 274*, 14434−14443.
32. Huang, C. K., Zhan, L., Ai, Y., and Jongstra, J. (1997) LSP1 is the major substrate for mitogen-activated protein kinase-activated protein kinase 2 in human neutrophils, *J. Biol. Chem. 272*, 17−19.
33. Blacklow, S. C., Raines, R. T., Lim, W. A., Zamore, P. D., and Knowles, J. R. (1988) Triosephosphate isomerase catalysis is diffusion controlled. Appendix: Analysis of triose phosphate equilibria in aqueous solution by ^{31}P NMR, *Biochemistry 27*, 1158−1167.
34. Cole, P. A., Burn, P., Takacs, B., and Walsh, C. T. (1994) Evaluation of the Catalytic Mechanism of Recombinant Human Csk (C-Terminal Src Kinase) Using Nucleotide Analogs and Viscosity Effects, *J. Biol. Chem. 269*, 30880−30887.
35. Cleland, W. W. (1986) Enzyme Kinetics as a tool for Determination of Enzyme Mechanisms, in *Investigations of rates and mechanisms of reactions* (Bernasconi, C. F., Ed.) 4th ed., Vol. 6, pp 791−870, Wiley-Interscience Publications, New York.
36. Johnson, L. N., Noble, M. E., and Owen, D. J. (1996) Active and inactive protein kinases: Structural basis for regulation, *Cell 85*, 149−158.
37. Smith, L., and Smith, J. B. (2002) Lack of constitutive activity of the free kinase domain of protein kinase C ζ. Dependence on transphosphorylation of the activation loop, *J. Biol. Chem. 277*, 45866−45873.
38. Cacace, M. G., Landau, E. M., and Ramsden, J. J. (1997) The Hofmeister series: Salt and solvent effects on interfacial phenomena, *Q. Rev. Biophys. 30*, 241−277.
39. Park, C., and Raines, R. T. (2001) Quantitative analysis of the effect of salt concentration on enzymatic catalysis, *J. Am. Chem. Soc. 123*, 11472−11479.
40. Wu, H., Zheng, Y., and Wang, Z. X. (2003) Evaluation of the Catalytic Mechanism of the p21-Activated Protein Kinase PAK2, *Biochemistry 41*, 1129−1139.
41. Trauger, J. W., Lin, F. F., Turner, M. S., Stephens, J., and LoGrasso, P. V. (2002) Kinetic Mechanism for Human Rho-Kinase II (ROCK-II), *Biochemistry 41*, 8948−8953.
42. Chen, G., Porter, M. D., Bristol, J. R., Fitzgibbon, M. J., and Pazhanisamy, S. (2000) Kinetic Mechanism of the p38-MAP Kinase: Phosphoryl Transfer to Synthetic Peptides, *Biochemistry 39*, 2079−2087.
43. LoGrasso, P. V., Frantz, B., Rolando, A. M., O'Keefe, S. J., Hermes, J. D., and O'Neill, E. A. (1997) Kinetic Mechanism for p38 MAP Kinase, *Biochemistry 36*, 10422−10427.
44. Segel, I. H. (1975) *Enzyme Kinetics: Behavior and Analysis of Rapid Equilibrium and Steady-State Enzyme Systems*, Whiely-Interscience, New York.
45. Cleland, W. W. (1979) Substrate Inhibition, *Methods Enzymol. 63*, 500−513.
46. Kravchuk, A. V., Zhao, L., Kubiak, R. J., Bruzik, K. S., and Tsai, M. D. (2001) Mechanism of Phosphatidylinositol-Specific Phospholipase C: Origin of Unusually High Nonbridging Thio Effects, *Biochemistry 40*, 5433−5439.
47. McKay, G. A., and Wright, G. D. (1996) Catalytic Mechanism of Enterococcal Kanamycin Kinase (APH(3′)-IIIa): Viscosity, Thio, and Solvent Isotope Effects Support a Theorell-Chance Mechanism, *Biochemistry 35*, 8680−8685.

BI050608Q